I.P.N. - 91406 ORSAY CEDEX

institut de physique nucléaire CNRS - IN2P3 UNIVERSITÉ PARIS - SUD

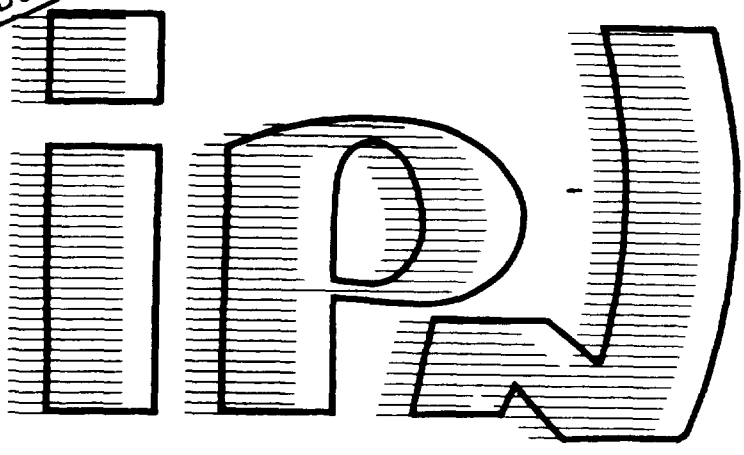

IPNO-DRE. 96-24

Onia, Open Heavy Flavours, meson decays and combinatorial effects in Muon Pairs Measurements, in ALICE at LHC

D.C. ZHOU*, D. JOUAN
Institut de Physique Nucléaire, B.P. n° 1,
F 91406 Orsay Cedex

IPNO-DRE. 96-24

Onia, Open Heavy Flavours, meson decays and combinatorial effects in Muon Pairs Measurements, in ALICE at LHC

D.C. ZHOU*, D. JOUAN
Institut de Physique Nucléaire, B.P. n° 1,
F 91406 Orsay Cedex

* On leave from the Institute of Particle Physics, Hua-Zhong Normal University, Wuhan, 430070, China

Onia, Open Heavy Flavours, meson decays and combinatorial effects in Muon Pairs Measurements, in ALICE at LHC

D.C. Zhou* D.Jouan
Institut de Physique Nucléaire, B. P. 1, 91406, France

Abstract

The ALICE collaboration has proposed to build a detector dedicated to nucleus-nucleus collisions at LHC. The aim is to study strongly interacting matter at extreme energy densities and particularly to search for evidence of the predicted QCD phase transition to quark-gluon plasma (QGP). The suppression of heavy quark resonances, J/ψ and Υ, is one of the most promising signatures of the quark-gluon plasma. This work gives out results of a simulation of signals and backgrounds in muon pairs measurements with a forward spectrometer, including the dimuon production from resonances, open charm, open beauty and meson decay in Pb-Pb, Ca-Ca and P-P collisions. The effect of the nature of the absorber on the mass resolution is discussed , and a comparison with measurement in the central region is also made.

*On leave from the Institute of Particle Physics, Hua-Zhong Normal University, Wuhan, 430070, China

Contents

1 Introduction

At CERN and BNL, energies of several tens or hundreds of GeV per nucleon have become available in the last ten years in heavy ion collisions, up to the heavier ions in the most recent period. The violence of these collision could be sufficient to form a state of nuclear matter with density of the order of nucleon density, and with an energy density corresponding to a temperature of the level of 150 MeV. QCD calculations predict[1] that a transition toward a deconfined state of matter, the plasma of quarks and gluons, should happen at this threshold value.

Around 2005 the Large Hadron Collider will deliver beams up to Pb, increasing the maximal energy available in nucleon nucleon collisions from 20 to 5500 GeV.

One of the most promising signatures for the existence of this new phase of matter is the suppression of heavy quark resonances (J/ψ,ψ', Υ, Υ' and Υ")[2][3][4]. Being very massive these pairs of quarks are produced at the beginning of the collision. They are then the most sensitive to the first stage of the collision, where the quark and gluon plasma could be formed.

Heavy quark (c,b) are indeed produced in hard scattering processes at the beginning of a nucleus-nucleus encounter, and a fraction of these quarks appears as bounded quarkonium resonances. The suppression of these resonances would be due to the Debye screening of the heavy quark pair potential in the plasma[2][3]. The screening radius in the medium is inversely proportional to the density of colour charges and to the energy density. If the screening radius is smaller than the size of a resonance, the confining force is screened and a bound state cannot be formed.

Because of the finite resonance formation time, high P_T ('fast') quark pairs can nevertheless escape the QGP unaffected, yielding a characteristic P_T independent suppression pattern. Heavy quark resonances then appear as the specific probes of the deconfining nature of the medium. Nevertheless it is noteworthy that dealing with a production mechanism which could vary when changing the entrance channel conditions, it is better to evaluate this suppression effect with respect to a reference produced by a similar mechanism, but insensitive to the deconfinement. At SPS energies, the production of high mass dimuons by direct quark antiquark annihilation is used. At higher energies it will be replaced by the continuum of the heavy quark pair production.

Several groups [5],[6] have carried out the measurement of dimuons at SPS energies, yielding in particular to high mass vectors J/ψ and ψ'. Resonances and reference are measured for different entrance channels, from p-nucleus to Pb-Pb, as a function of their transverse momentum and with respect to the transverse energy produced in the heavy ion collision.

At LHC, the ALICE experiment[7][8] will be the detector dedicated to the study of nucleus-nucleus collision. The collision from Pb+Pb at 5.5 TeV will lead[9] to energy densities beyond 7 Gev/fm^{-3}, and the system will then stay above the threshold of QGP formation in a much longer period than at the SPS, and in a larger volume. QGP formation will then be more probable and more measurable at LHC. The Υ

family will become available[3], and the open beauty and charm will also furnish an ideal references[10][11]. In its letter of intent the ALICE detector was considering measurement of hadrons and electrons with a low Pt threshold in the central rapidity domain. The ALICE collaboration has been requested by the LHC comitee to look for a possibility to include also muons measurement in the set up. This work is part of the effort made in the ALICE dimuon study group between 1993 and 1995 leading to the submission of the project of forward muon arm[4][8][12].

2 Muon Detector

2.1 Global Overview

The basic requirements of the dimuon measurement are the following:

- The mass resolution should be close to 100 MeV in order to separate Υ' from Υ".
- The background from pions and kaons decays should be as low as possible.
- The particle densities behind the absorber must not exceed 10^{-2}particle/cm $^{-2}$.

The second requirement implies to use a thick absorber as close as possible to the interaction point, and will also benefit of the measurement at high rapidities,where the decay lengths are increased.

The principle lay-out of the forward muon spectrometer is shown in fig 1 . The basic components are a front hadron absorber, a small angle absorber along the beam, a dipole magnet, tracking chambers and a muon filter followed by the trigger chambers.

The global view of the ALICE detector is shown in figure 2.

2.2 Mass Resolution and Absorber

In order to decrease the particle densities down to 10^{-2} cm^{-2}, a 10 interaction lenghts absorber is considered[4][13][14][16]. The effect of the absorber is a major ingredient of the mass resolution, through multiple scattering and straggling of the energy loss suffered by the muons. Part of the multiple scattering can be corrected using the interaction point and the exit point from the absorber. The efficiency of this correction is sensitive to the distance between the absorber and the interaction point.

The effect of the energy straggling, which cannot be corrected, increases proportionally to the square root of the ratio between the interaction length and the radiation length, and for a given number of interaction lengths, it increases by a factor 3.6 between C and W. The effect on the momentum precision depends on the angle, since the average momentum increases for smaller angles.

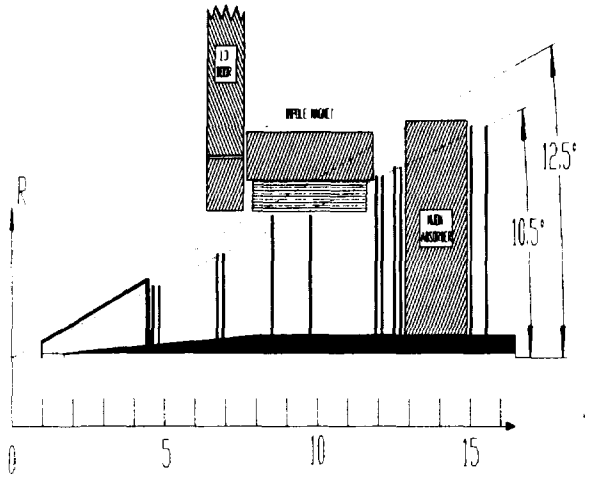

Figure 1: *principle layout of upper part of the forward muon detector, including: absorber, small angle absorber, dipole magnet, tracking chambers, muon filter and trigger chambers.*

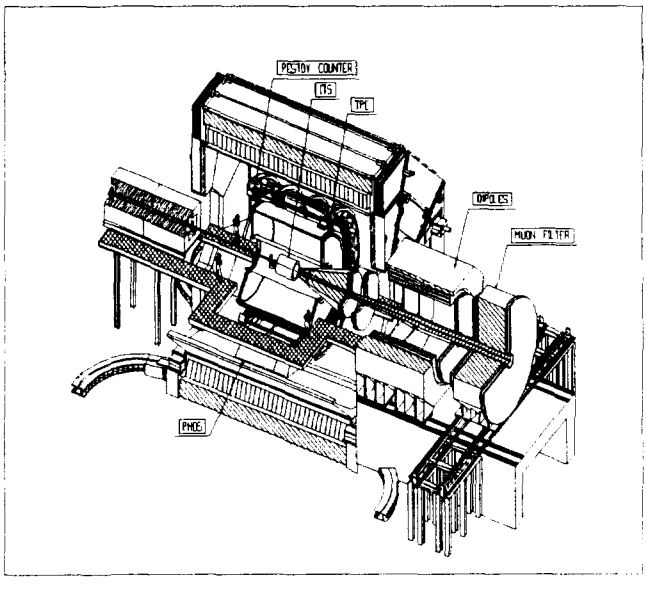

Figure 2: *The global view of the muon arm in ALICE detector*

The figure 3 4 displays the results of a Monte Carlo calculation for the Υ family using carbon and tungsten absorber. After generation of muon pairs using the kinematical distributions that will be introduced in a forthcoming section, the effects of the multiple scattering are associated to each muon, thanks to software tools from the NA38 experiment, which have then been found to reproduce experimental data. A comparison with GEANT has also been done in the past. The average energy loss is corrected, and the angular deviation is corrected thanks to a software developped by HELIOS. The simulation takes also into account the effect of the tracking, as it has been estimated[15] as a function of the muon angle and momentum, assuming 50 μm precision on the track measurement before and after the magnet, and an homogeneous dipolar field (B=0.7T, 3m length). On the average, the effect is a momentum resolution of 0.7%, as shown in the figure, which also displays the various contribution to the uncertainty on the muon momentum measurement. The dotted line in the plot of scattering angles corresponds to the remaining diffusion after corrrection.

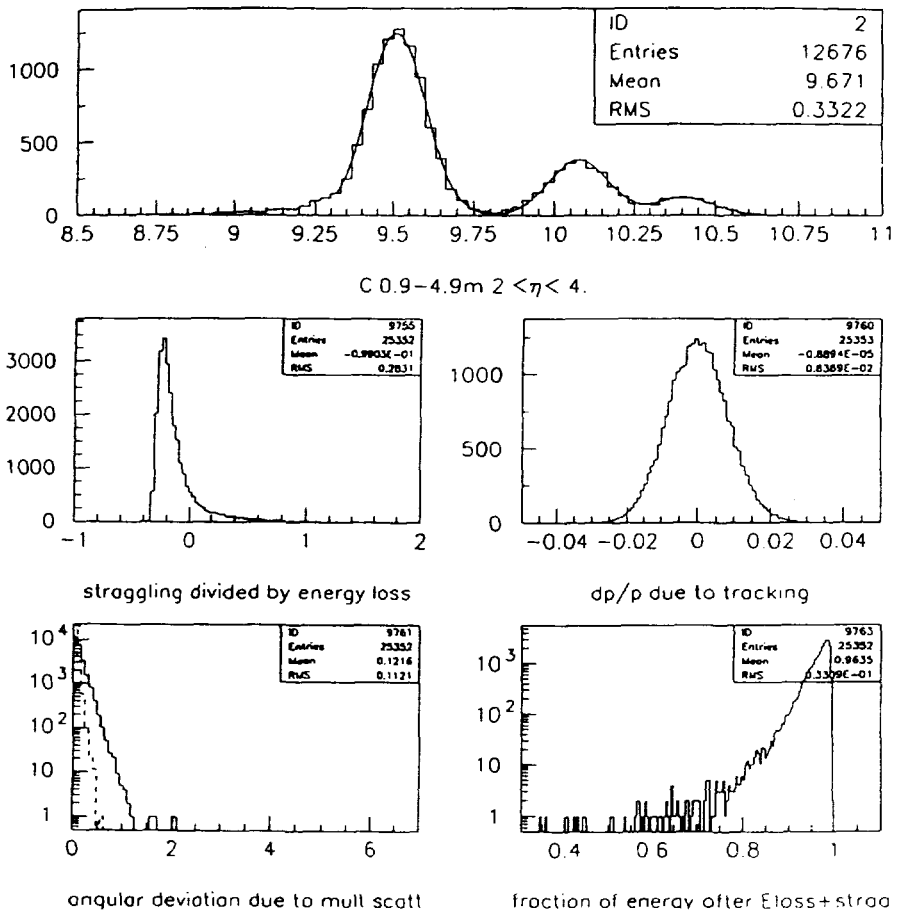

Figure 3: *The effect from multiscattering and energy loss and their correction for* Υ *using 4m C absorber starting at 0.9 m from the interaction point*

We estimate the mass resolution in the distributions obtained for the Υ family, thanks to a fit with three gaussians. In this fit, the relative positions are fixed according to the masses of Υ,Υ, and Υ'', and the resolution is the common width (P4) of the gaussians, with free amplitudes P1,P2 andP3 .

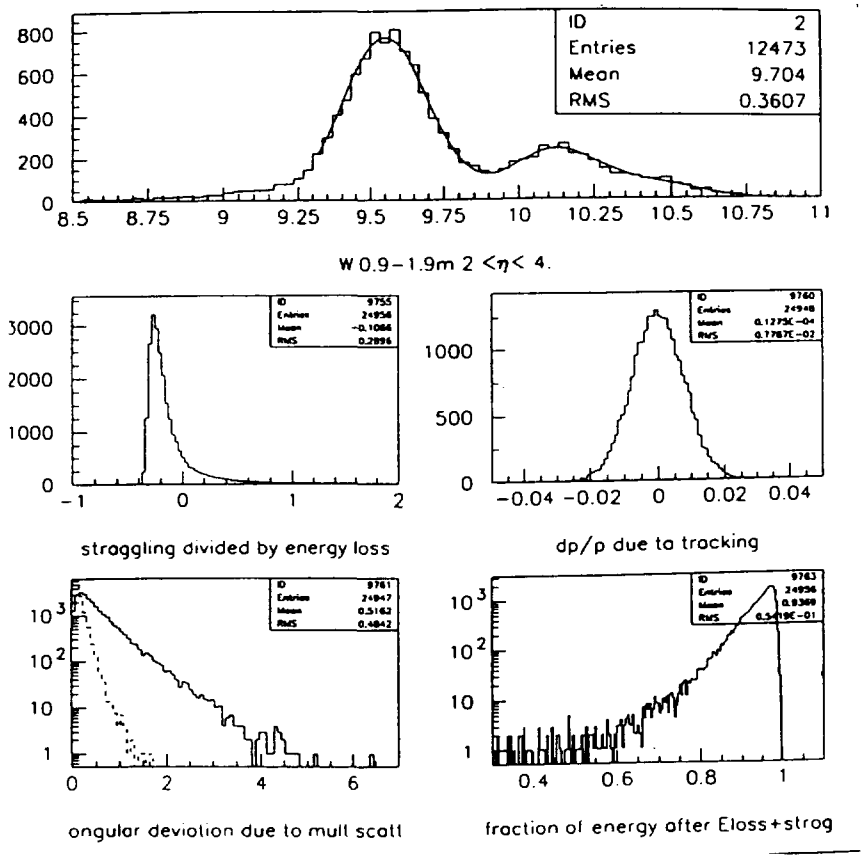

Figure 4: *The effects of multiple scattering and the corrections for* Υ *using 1m W absorber starting at 1m from the interaction point*

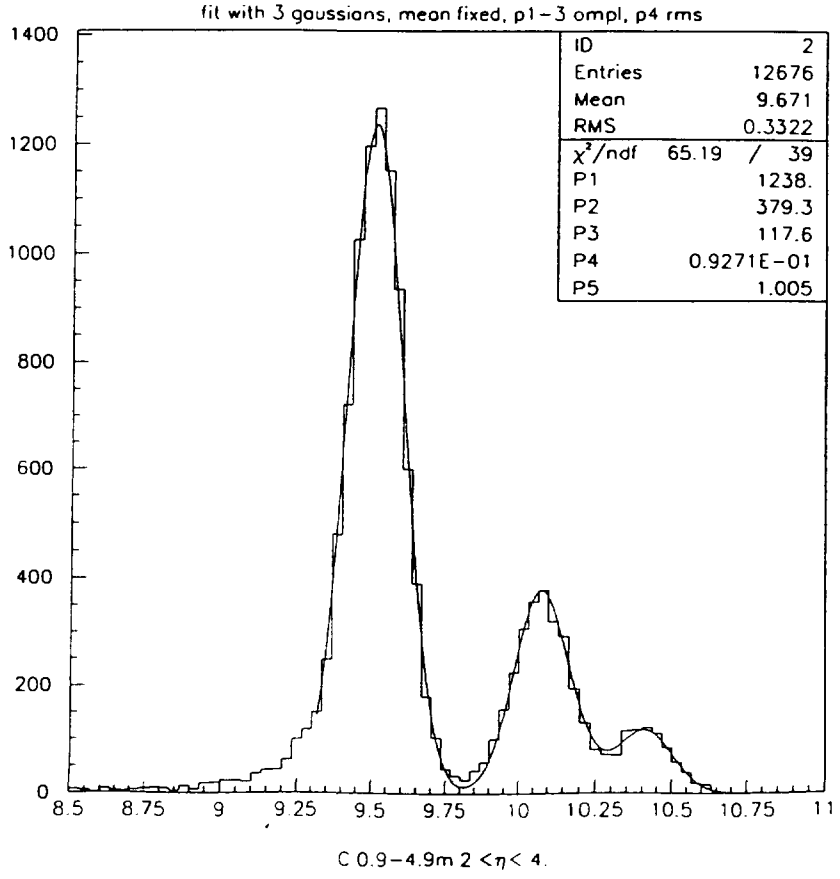

Figure 5: *resolution with 4m absorber C at 0.9 m from interaction point*

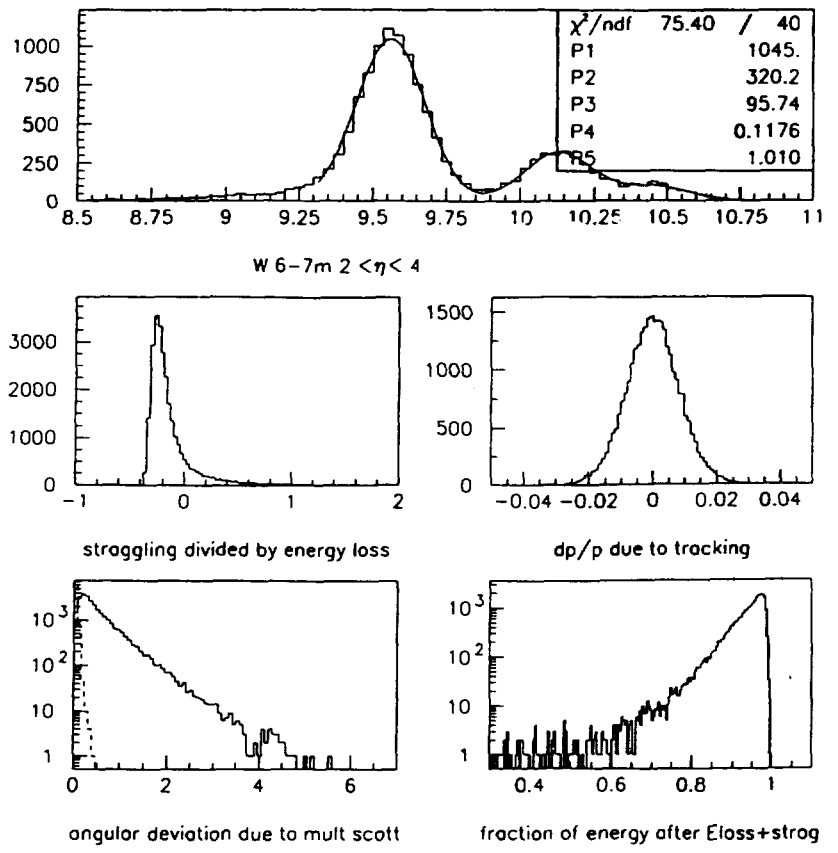

Figure 7: *resolution with 1 m absorber W at 6m from interaction point*

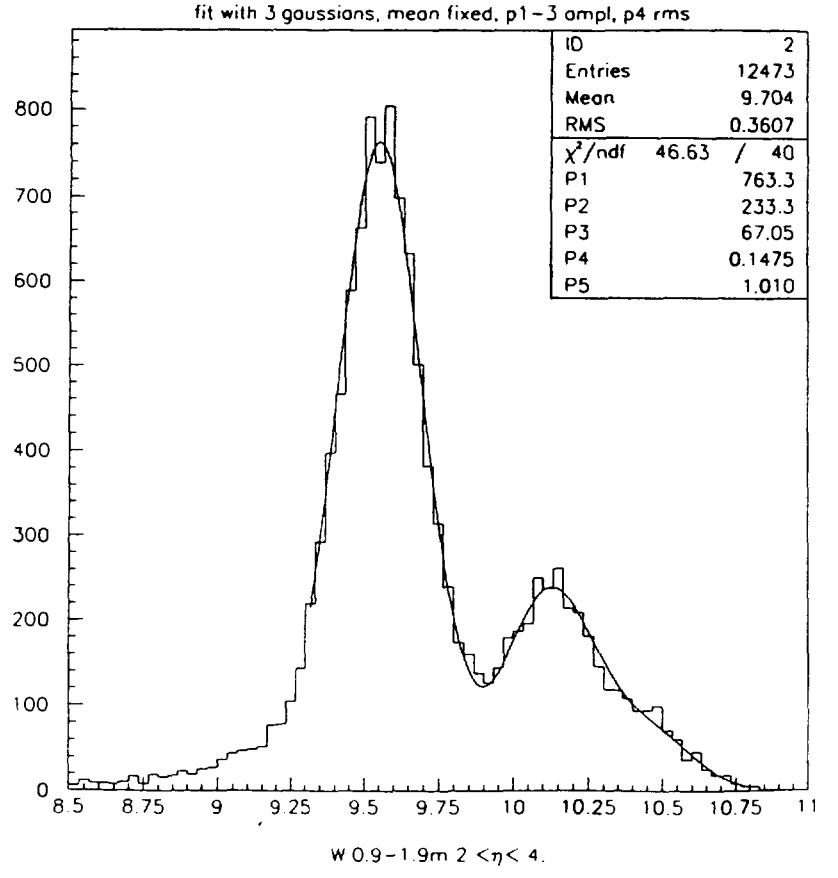

Figure 6: *resolution with 1 m absorber W at 0.9 m from interaction point*

In order to minimize the number of hits in the chambers downstream to the absorber, a layer of W is considered after the carbon absorber[13].

We see that:

1. the 4m C absorber starting at 0.9 m from the interaction point leads to a 1% precision and 1m W to 1.5%, as expected.

2. 1m W absorber starting at 6m from the interaction point and 4m C absorber starting at 0.9m from the interaction point lead to approximate values of the resolution. A layer of 5cm of W at the end of the absorber will then be very useful for reducing the number of hits in the chambers[13], without spoiling the resolution.

3. 1% resolution allows to determine Υ, Υ', and Υ'' amplitudes, which are found in the ratio $1 : 0.3 : 0.095$ when the generation values were $1 : 0.3 : 0.1$.

3 Simulation of the Signal and the Background for Dimuon Production

3.1 Basic Ideas used for Muon Pairs Production

Several programs have been considered in the working group[13][14][16] for dimuon measurement at ALICE. In this report, we will focus on the results obtained with a simplified program aiming at the estimates of the dimuon production with high statistic in a reasonable computing time. The goal was to obtain a tool for optimizing the main parameters of the absorber, and the location and aperture of the detector. It is noteworthy that a significant contribution from meson decays to the tail of the distribution of background is very difficult to obtain using GEANT, due to the computing time of the shower. For these small probabilities, another solution must be find.

In order to simplify the treatment, we only apply the prevailling trends of the phenomenon, for intance the decays of open b and c or of light mesons are schematically considered as compared to elaborated code such as GEANT or PYTHYA and JETSET or HIJING.

Structure functions are not considered in the program, but the kinematical distributions coming from dedicated theoretical codes are used, which is in a way more flexible.

This program include: - The signal generator for J/ψ and Υ family, - Open charm and open beauty generators, - Drell-Yan generator, - pion and kaon generator, - and combinatorial analyse section.

Such a simple code allows to consider that each particle decays as a muon, using the probability as a weight, which is an important saving of time for small probabilities. The various components are mixed into events, following poissonnian multiplicities, and pairs are then built on an event by event basis. Such a program can be used to simulate and to analyze the dimuon production from P-P to A-A collisions. It also could be convenient for testing analyzing techniques, combinatorial problems,

	$\Upsilon_{\mu\mu}$	$J/\psi_{\mu\mu}$	$b\bar{b}$	$c\bar{c}$
σ_{pp}	12.75 nb	4.72 μb	85 μb	1.07 mb
$pp \rightarrow AA$	$A^{1.9}$	$A^{1.8}$	$A^2/2$	$A^2/2$
central coll. prob.	0.1			
enrichment factor	5			

Table 1: onium and heavy quarks cross sections in pp collisions at 5.5 TeV center of mass energy (one hemisphere), and extrapolation used between pp and AA collision

$Centr.colli.$	$Br_{\rightarrow\mu\mu}\sigma_{\Upsilon}$	$Br_{\rightarrow\mu\mu}\sigma_{J/\psi}$	$\sigma_{b\bar{b}}$	$\sigma_{c\bar{c}}$
$Pb-Pb$	162. μb	35. mb	0.9 b	11.6 b
$Ca-Ca$	7. μb	1.8 mb	34 mb	428. mb
$P-P$	32. nb	12. μb	212. μb	2.7 mb

Table 2: onium and heavy quarks cross sections for Pb-Pb, Ca-Ca and P-P central collisions at $\sqrt{s}$ = 5.5 TeV, 7 TeV and 14 TeV respectively (one hemisphere)

background subtraction techniques, etc..

3.2 Cross Section

The expected cross section is the most basic question related the experimental measurement for the signal and the background. Up to SPS energies, the continuuum and resonances production of high mass dimuon displays an experimental scaling behaviour[17][18] with respect to $\sqrt{\tau}$=M/$\sqrt{s}$. Such a low energy exponential parametrization leads to a saturation of the cross section at high energy. This ignores the effects of the structure function of relevance for $Y > 4(10^{-5} < x < 10^{-3})$, which are expected to create an increase of the production as a function of the energy [19],[20].

The onium and heavy quarks cross sections in pp collisions at 5.5 TeV center of mass energy that we consider are shown in tab 1. They range in the domain expected by [11][20][21][22].

The extrapolations of the cross section from pp to AA collision are taken from SPS and Fermilab results for heavy resonances production, roughly of the A^2 type, and from HIJING for light mesons, which appear to behave proportionally to A. The extrapolations used for Υ,J/ψ, b$\bar{b}$ and c$\bar{c}$ are shown in table 1. From usual geometrical models, 50% of hard probes production is located in 10% most central collisions due to this A^2 behaviour. As far as Pb and Ca collisions are concerned, we will consider only these central collision in the following. This leads to the cross section of onium and heavy flavor production of table 2. Table 3 shows the total central cross section and the multiplicities of onium and heavy pairs.

$Centr.colli.$	σ_{tot}	$N_{\Upsilon\to\mu\mu}$	$N_{J/\psi\to\mu\mu}$	$N_{b\bar{b}}$	$N_{c\bar{c}}$
$Pb-Pb$	550 mb	2.9 10^{-4}	0.64	1.64	21.7
$Ca-Ca$	300 mb	2.3 10^{-5}	6. 10^{-3}	0.11	1.43
$P-P$	100 mb	3.2 10^{-7}	1.2 10^{-4}	2.1 10^{-3}	2.68 10^{-2}

Table 3: total central collision cross section and the number of onium and heavy flavor pairs per central collisions at $\sqrt{s}$ = 5.5 TeV, 7 TeV and 14 TeV respectively (one hemisphere)

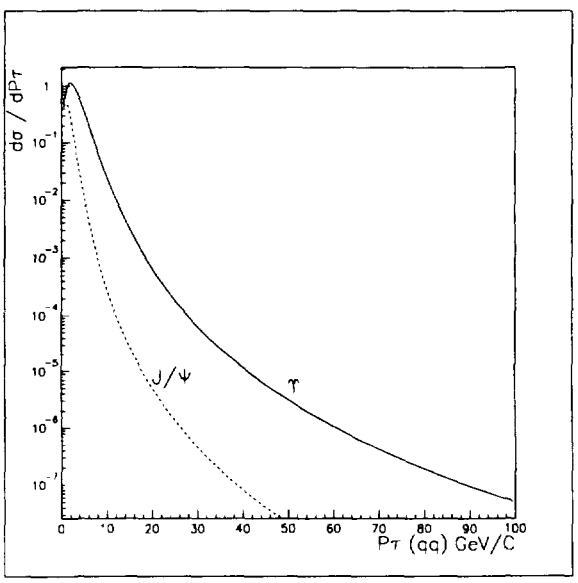

Figure 8: transversal momentum distribution for resonances J/ψ and Υ at 5.5 TeV

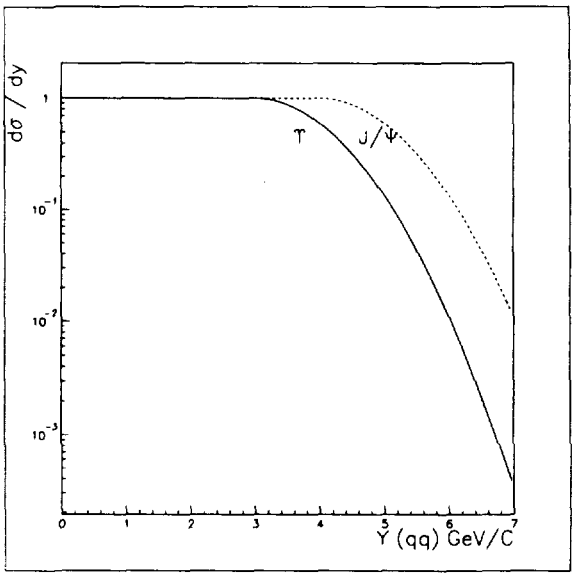

Figure 9: rapidity distribution for resonances J/ψ and Υ at 5.5 TeV

3.3 Kinematical Distribution of Signal and Background

- **J/ψ and Υ**

Concerning the resonances J/ψ and Υ a Breit-Wigner parametrization of the mass distribution is considered. The relative abundances considered are 1:0.01 for J/ψ and ψ' and 1:0.3:0.1 for Υ, Υ' and Υ". The cross section of onium production for J/ψ and Υ family produced in P-P and A-A collision have been listed in table 2. The rapidity distribution for J/ψ and Υ families are flat with a gaussian tail of width unity centered respectively at 4. and 3. (figure 9). The transversal momentum distributions for J/ψ family and Υ are displayed figure 8, where the following parametrizations have been used:

$$\frac{d\sigma_{J/\psi}}{dP_T} \propto \frac{P_T}{[1+(P_T/2.3)^2]^{3.5}} \tag{1}$$

$$\frac{d\sigma_{\Upsilon}}{dP_T} \propto \frac{P_T}{[1+(P_T/4.7)^2]^{3.5}} \tag{2}$$

- **Open Charm and Open Beauty**

At LHC energy, open charm and open beauty will be the predominant sources of dimuon production. They will give the most important contribution to the combinatorial background, but the high mass part will also be the reference for the measurement of resonances suppression.

In order to simulate $b\bar{b}$ and $c\bar{c}$ production, we have considered the mass distribution predicted by Gavai et al[22] using $MRSD'$ structure function. Figure 10(a,b,c) shows the shape that we have considered. It is noteworthy that these distributions must be normalised to the multiplicities of quarks pairs presented in table 3, i.e. 1.7 for $b\bar{b}$ and 21.7 for $c\bar{c}$ in one hemisphere for PbPb central collision. With such a normalisation the high mass parts of the two distributions compare within a factor 2.

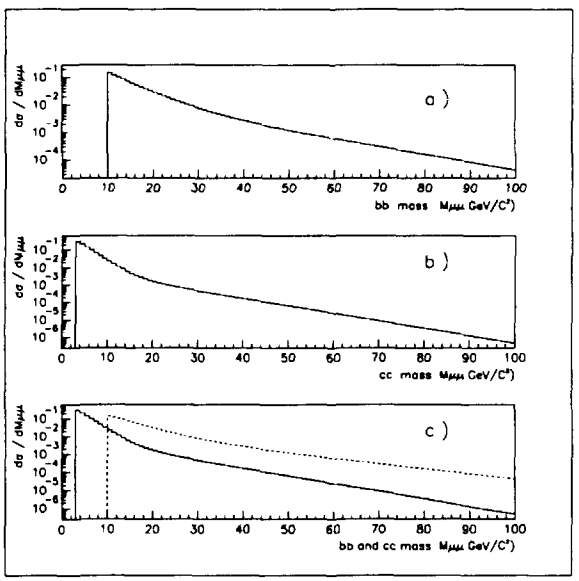

Figure 10: mass distribution considered for open beauty $b\bar{b}$ (a), open charm $c\bar{c}$ (b) and their comparison (c) at 5.5 TeV (A.U., no relative normalisation)

The rapidity and transversal momentum distributions are taken similar to the one of Υ and J/ψ, which is in qualitative agreement with [11][22]. Momenta of the two quarks are deduced from the kinematical variables of the pair and from the random choice of three additionnal angles. The fragmentation of c and b quarks are taken into account through a parametrization according to [23] (see figure 11). The muon is then deduced thanks to a three-body semileptonic decay along $b \rightarrow \mu + \nu + c$ and $c \rightarrow \mu + \nu + s$ in the center of mass of the pair, with branching ratios 0.1 and 0.14 respectively.

- **Hadron π and k Decay**

At SPS energies, decays from these light mesons are the main contribution to combinatorial background. Open heavy flavour decays will be predominant at LHC, specially in the forward region choosen for the ALICE muon arm. This will allow a direct access to this production through high mass continuum where the contribution from π and k decays will be negligible.

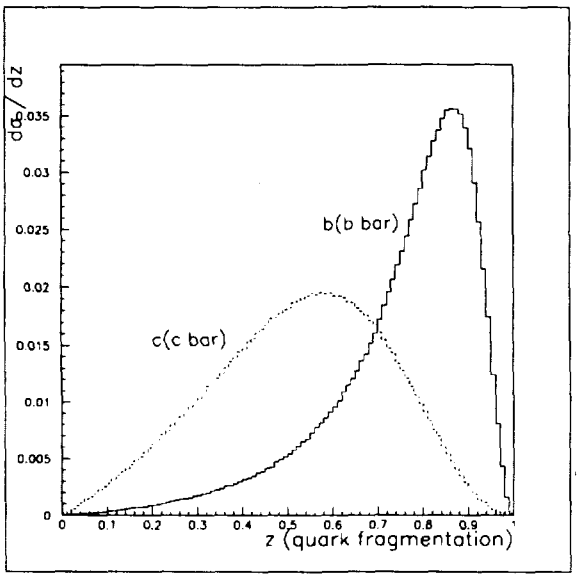

Figure 11: quark fragmentation distribution

In case of the Pb+Pb central collisions we have simulated the muon production from π and k decay using a two gaussian parametrization[16] of the rapidity distribution of the mesons (figure 12(a,b)) simulated with HIJING.

$$\frac{dN_\pi}{d\eta} \propto \alpha_1 exp[-\frac{|\eta - 0.22|^2}{2 * 1.47^2}] + \alpha_2 exp[-\frac{|\eta - 3.66|^2}{2 * 1.51^2}] \tag{3}$$

$$\frac{dN_k}{d\eta} \propto \alpha_3 exp[-\frac{|\eta - 0.79|^2}{2 * 1.54^2}] + \alpha_4 exp[-\frac{|\eta - 4.09|^2}{2 * 1.40^2}] \tag{4}$$

α_1=4913, α_2=1819, α_3=497.6, α_4=215.6. The number of charged hadron per unit rapidity at central rapidity is about 6000. The relative abundance considered for π and k is 1:0.11.

Transverse momentum distribution of π have been deduced from CDF results[24], the kaon distributions are deduced from them thanks to the parametrizations of Bourquin and Gaillard[25]. These distributions are displayed in figure 13.

$$\frac{dN_\pi}{dP_T} \propto P_T exp(-\frac{M_T}{0.16}) \qquad for P_T < 0.5 \tag{5}$$

$$\frac{dN_\pi}{dP_T} \propto P_T exp(-\frac{M_T^\pi}{(1.3 + P_T)^{8.28}}) \qquad for P_T > 0.5 \tag{6}$$

$$\frac{dN_k}{dP_T} \propto [\frac{\sqrt{P_T^2 + 0.018215} + 2.}{M_T^k + 2}]^{12.3} \bullet \frac{dN_k}{dP_T} \tag{7}$$

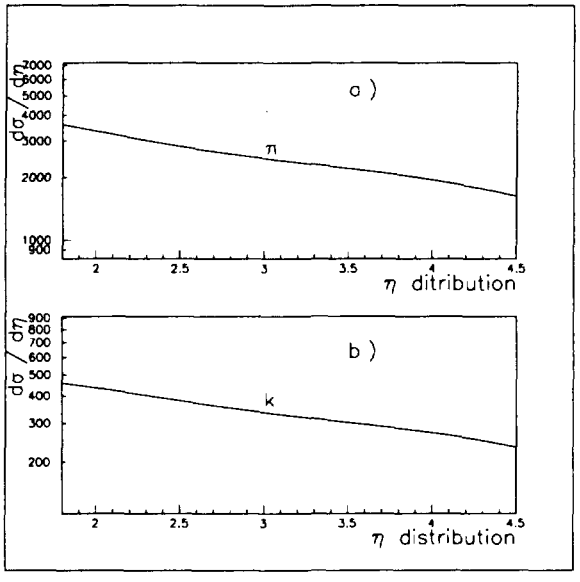

Figure 12: rapidity distribution of charged hadrons π a) and k b)

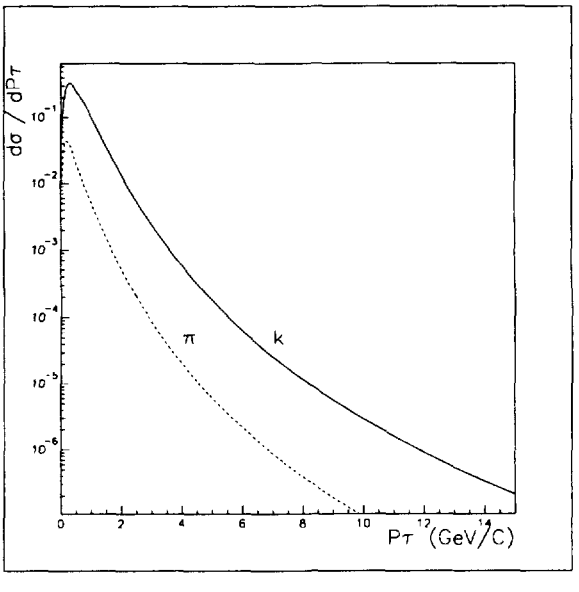

Figure 13: transversal momentum distribution for π and k

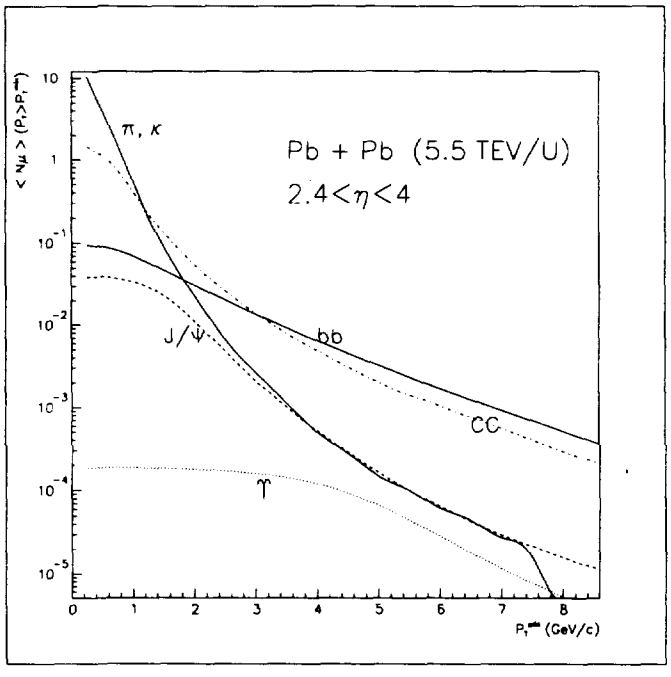

Figure 14: average muon rate per event as a function of a transversal momentum $P_{T_{min}}$ threshold for Pb-Pb collision at 5.5 TeV .

The position of the decay of the meson into muon is randomly choosen along the survival probablity of the primary particle in the absorber, with an associated weight allowing to reproduce the probability in the event. Thanks to the use of the weight, every meson giving a muon inside the acceptance of the spectrometer can be kept.

For all the dimuon sources, the muons are then followed in the absorber where they suffer multiple scattering effects. Energy loss and angular deviation are corrected as for real data, as explained in a previous section.

4 Simulated Results for Signal and Background productions

4.1 Rates of Muon production

In figure 14 15 16 are shown the main sources of muon production in Pb-Pb, Ca-Ca and P-P collisions, as a function of the transversal momentum threshold $P_{T_{min}}$, in the forward region between in rapidity 2.4 to 4.. These rates are also presented in table 4.

The muon production from π and k decays is the most important, which makes putting an absorber as close as possible to the collision point mandatory. Therefore the decay-in-flight of pions and kaons has been simulated under the assumption of 0.9 m decay length which corresponds to the closest distance of the absorber to the

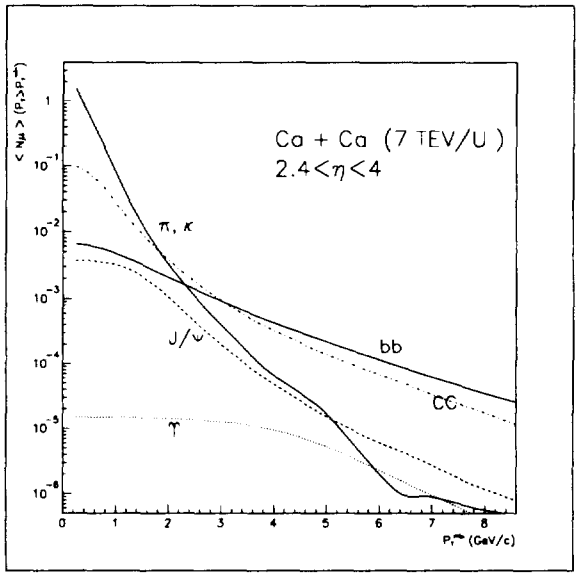

Figure 15: average muon rate per event as a function of a transverse momentum $P_{T_{min}}$ threshold for Ca-Ca collisions at 7 TeV.

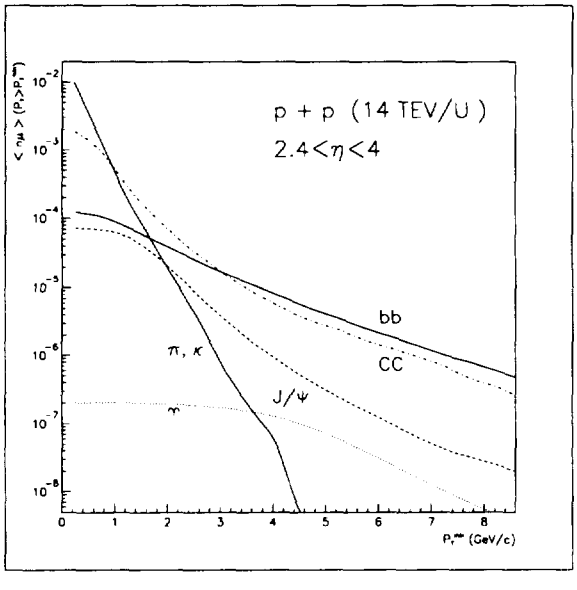

Figure 16: average muon rate per event as a function of a transverse momentum $P_{T_{min}}$ threshold for P-P collisions at 14 TeV.

coll.	P_t^{min}	Υ	J/ψ	bb	cc	decays	TOT
PbPb	0.	0.00019	.04	.095	1.45	10.58	13.02
	.5	0.00019	.04	.082	0.74	1.70	2.56
	1.	0.00018	.03	.058	.24	.24	.55
	2.	0.00017	.007	.025	.037	.016	.085
	3.	0.00015	.0014	.011	.010	.0022	.025
	4.	0.0001	.00038	.0054	.0039	.00046	.010
	5.	0.00005	.00013	.0028	.0017	.00014	.005
	6.	0.00002	.000055	.0015	.0009	.00006	.0025
CaCa	0.	0.000015	.0036	.0064	.1	1.61	1.72
	.5	0.000015	.0035	.0055	.05	,26	.32
	1.	0.000014	.0027	.0039	.015	.037	.059
	2.	0.000014	.00069	.0017	.0026	.0023	.0073
	3.	0.000012	.00013	.00075	.0007	.00033	.0019
	4.	0.000008	.000035	.00036	.00026	.00006	.00072
	5.	0.000004	.00001	.00019	.0001	.000016	.00033
	6.	0.000002	.000005	.00010	.00006	.000002	.00019
pp	0.	$2\ 10^{-7}$	$7\ 10^{-5}$	$1.2\ 10^{-4}$	$1.8\ 10^{-3}$	$9.9\ 10^{-3}$	$1.2\ 10^{-2}$
	0.5	$2\ 10^{-7}$	$7\ 10^{-5}$	$1\ 10^{-4}$	$9.5\ 10^{-4}$	$1.5\ 10^{-3}$	$2.6\ 10^{-3}$
	1	$2\ 10^{-7}$	$5.5\ 10^{-5}$	$7.3\ 10^{-5}$	$3\ 10^{-4}$	$2.2\ 10^{-4}$	$6.5\ 10^{-4}$
	2	$1.9\ 10^{-7}$	$1.4\ 10^{-5}$	$3.1\ 10^{-5}$	$4.5\ 10^{-5}$	$1.3\ 10^{-5}$	$1.0\ 10^{-4}$
	3	$1.6\ 10^{-7}$	$2.5\ 10^{-6}$	$1.4\ 10^{-5}$	$1.5\ 10^{-5}$	$5.7\ 10^{-7}$	$3.2\ 10^{-5}$
	4	$1.2\ 10^{-7}$	$7\ 10^{-7}$	$7\ 10^{-6}$	$5\ 10^{-6}$	$5.0\ 10^{-8}$	$1.3\ 10^{-5}$
	5	$6\ 10^{-8}$	$2.4\ 10^{-7}$	$3.5\ 10^{-6}$	$2\ 10^{-6}$	0	$5.8\ 10^{-6}$
	6	$2.5\ 10^{-8}$	$1.1\ 10^{-7}$	$1.9\ 10^{-6}$	$1\ 10^{-6}$	0	$3\ 10^{-6}$

Table 4: average rates of muons in central PbPb ,CaCa and pp collision, in the acceptance of the spectrometer

$P_T^{min}(GeV/c)$	1.	3.
$Pb-Pb$	0.15	$3.\ 10^{-4}$
$Ca-Ca$	$2.3\ 10^{-3}$	$2.8\ 10^{-5}$
$P-P$	$1.5\ 10^{-5}$	$5.\ 10^{-7}$

Table 5: total muon pair probability per event as a function of a transverse momentum threshold $P_{T_{min}}$ for Pb-Pb, Ca-ca and P-P collision at 5.5 TeV, 7 TeV and 14 TeV, accepted (angles and absorber) by the spectrometer.

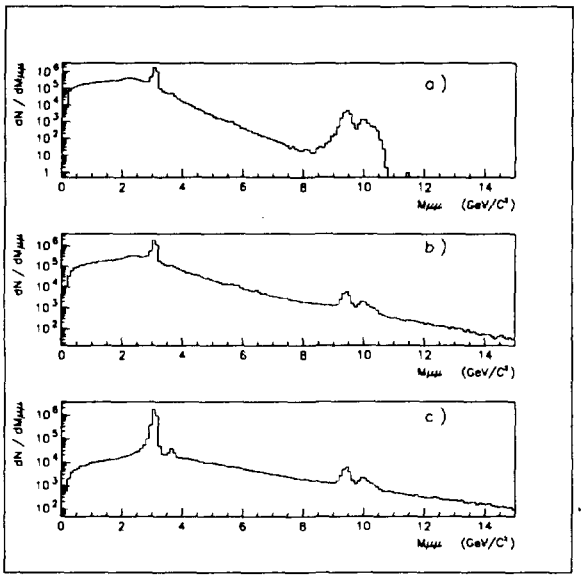

Figure 17: *a*). comparison between resonances and combinatorial background dimuons from π, k decays; *b*). comparison between resonances and combinatorial background spectrum of dimuon from open charm $c(\bar{c})$ decays; *c*). comparison between resonances and combinatorial background spectrum of dimuon from open beauty $b(\bar{b})$ decays

interaction region. In the range of $1 \sim 2$ GeV/c the decays from π, k and charm are very important. A cut $P_T > 1$ GeV/c exclude $\sim$ 90% of low transversal momentum muons from the hadron decays, $\sim$ 85% from $c\bar{c}$ decay , 40 $\sim$ from $b\bar{b}$ decay. When applying the cut $P_T > 3$ GeV/c, it will exclude $\sim$ 99.8% of muons from the π , k decays , $\sim$ 99% from $c\bar{c}$ decay , $\sim$ 88% from $b\bar{b}$ decay in experimental conditions. These cuts will be affected by the efficiency of trigger which will make them less selective.

The average number of pairs, which will be otherwize on the level of 100, is shown in table 5 for two values of the transverse momentum threshold corresponding to the selection of the J/ψ and of the Υ.

4.2 Mass Spectrum and Sensitivity of Signal/Background

In the following we consider the Pb-Pb case which is the most critical regarding the combinatorial production of muon originating from decays of mesons but also of open heavy flavours.

The statistical significance of dimuon production depends strongly on the acceptance of the dimuon spectrometer. We have studied the effects of the acceptance change. Considering an external angle of 15°, The production of dimuon decreases by 56% for J/ψ, by 53% for Υ, when we change the internal angle from 1° to 3°, (corresponding to η from 4.7 to 3.6). When fixing the internal angle at 2°, and changing the external angle from 10.5° to 15°, the production of dimuon increase by 28% for J/ψ, 32% for Υ but the sensitivity S/B decrease by 10% for Υ and 38% for J/ψ because

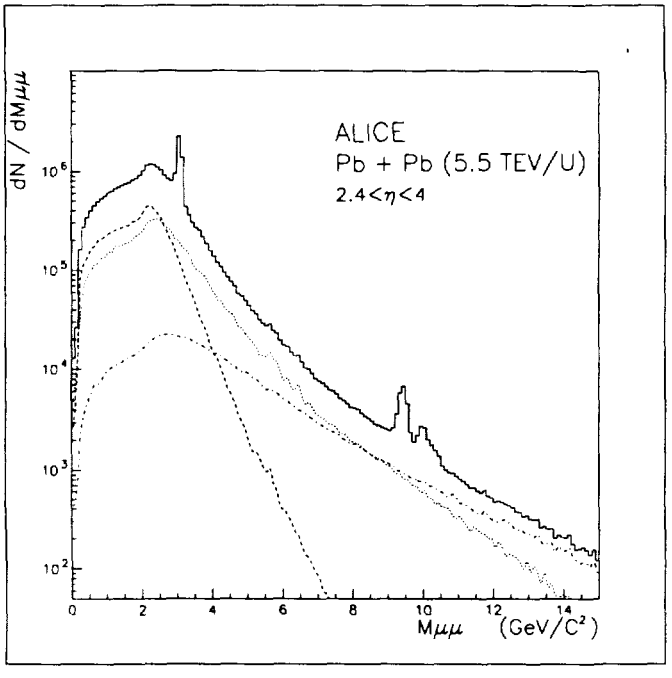

Figure 18: muon pairs mass spectrum including all sources in Pb-Pb collisions with $\sqrt{s} \sim 5.5$ TeV, for 1 month run, with $P_t^{\mu} < 1 GeV/c$. solid line $\rightarrow$ all measured pairs ; dashed line $\rightarrow \pi, k$ decays; dotted dashed linr $\rightarrow c\bar{c}$ decays; dotted line $\rightarrow b\bar{b}$ decays

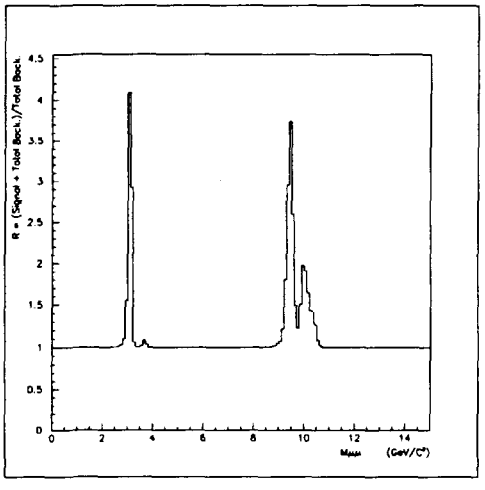

Figure 19: ratios of distribution for global dimuon and continumm background

contributions from hadron decays are increasing in this last case.

According to the design[12] of the muon arm, the available measured range for dimuon production will be limited in the range $2° \sim 10.5°$ which corresponds to the pseudo-rapidity region $2.4 < \eta < 4$. We first concentrate on the comparison between the resonances and the background from π and k decays. The figure 17 *a* shows the invariant mass spectrum of dimuon production with a transversal momentum cut for single muon $P_T > 1$ GeV/c. The combinatorial background from π and k decays decreases at high masses of muon pair. In the J/ψ mass range, a peak of J/ψ resonance is appearing clearly. The value of ratio between signal J/ψ and background muon pair is ~ 7.26. In higher mass region the background below the Υ is negligible, thanks to the forward kinematical effect.

The comparisons between the resonances and background from $c\bar{c}$ and $b\bar{b}$ semileptonic decays are shown in figure 17 b and c. Contributions to the continuum come from correlated pair, but also from uncorrelated ones. Contributions from $c\bar{c}$ and $b\bar{b}$ have the same magnitude in the Υ range and are more important than the one from π and k decays.

The overall mass spectrum of muon pairs is shown in figure 18 for Pb-Pb. It takes into account combinatorial pairs between different sources, not only between muons of same origin. The ratio of total muon pair production to the continuum, essentially of combinatorial nature, is displayed in figure 19, showing a rather good sensitivity to the resonance production in spite of the important continuum increase due to these combinations between all sources .

Figure 18 show that, for Pb-Pb at LHC energies, the contribution from π, k (dashed line) and open charm (dotted dashed line) decays are important in the region $0 < M_{\mu^+\mu^-} < 2.5$ GeV/c, whereas at higher masses the relative contribution from π, k decays decreases rapidly. Open charm decays will be the larger source of muons

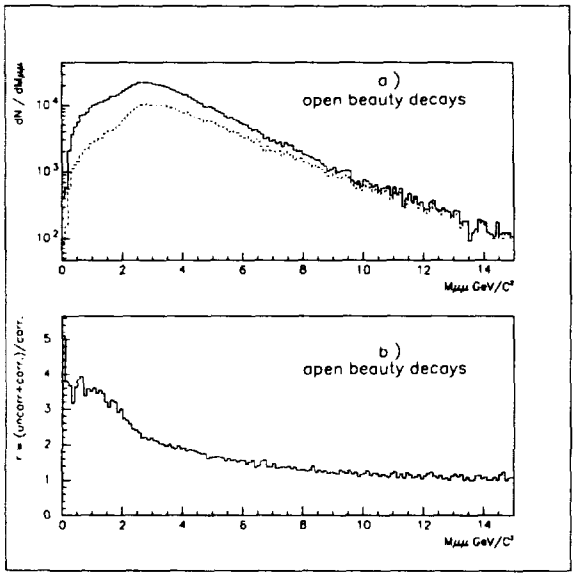

Figure 20: comparison between the distributions for the correlated and mixed muon pair from $b\bar{b}$ decay for Pb-Pb collisions at 5.5 TeV

feeding this intermediate region, but they will be combinatorially mixed with the other sources in such a way that it will be impossible to disentangle them on a purely experimental basis.

So far the continuum then contains very important informations, the open heavy flavour production that is the ideal reference for Debye screening studies, but available in an indirect form, since, in order to extract it, the dimuon production must be interpreted through models including production of the various sources and combinatorial building of the pairs measured in each collision. This is a potential source of important systematic biases.

In this context the very high mass domain, beyond the Υ, appears very promising since this simulation suggests that the open beauty production should be dominant.

An even more interesting observation can be made when comparing the mass spectrum of muon pairs originating from one $b\bar{b}$ pair ("true pair") to the one containing also the combinatorial pairs of muons, coming from different quark pairs. Figure 20 shows that this last component is vanishing for high masses, and it then finally appears that, contrarily to the rest of the spectrum, the very high mass part shoud be a rather pure $b\bar{b}$ contribution, even free of combinatorial complications, directly comparable to the same production in pp and CaCa production and to the Υ production.

As an academic exercice in order to verify the origin of this interesting effect, we use a simple model of the formation of correlated and mixed(correlated+uncorrelated) muon pairs. Having in mind the simplified picture of a pair whose mass is roughly the sum of the transverse momenta of the two muons, we simply assume a poissonian distribution of pairs, with an associated variable x exponentially distributed (see figure

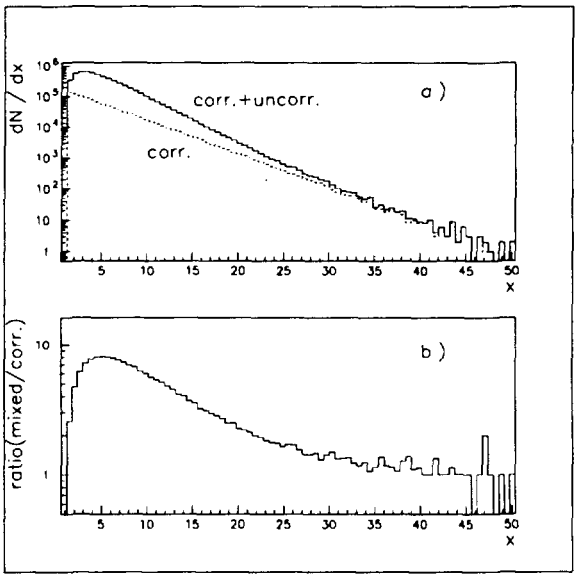

Figure 21: the distribution and their ratios for correlated and mixed variables

21 a). From x, we randomly get two values x_1 and x_2, gaussianly distributed with the condition $x_1+x_2 = x$. The x_1 and x_2 set of values obtained this way form the true pairs, from which one can build also the uncorrelated pairs and the associated new x values, inside "events" consisting of random numbers of pairs distributed along a poisson law. Figure 21 shows that, apart from the effect of the low Pt cut, the distribution obtained this way are very similar to the one coming from the open beauty decay into muons (figure 20).

Finally, for the sake of completeness, figures 22 to 25 display the rapidity and transverse momentum measured distributions of the various muon pair sources, with the two typical Pt cuts foreseen for the trigger.

In order to study quantitatively the sensitivity of rate of signal(S) and combinatorial background(B), we consider the number of dimuons in the region ($\pm 100 MeV$) of the J/ψ and Υ family, in accordance with the 100 MeV mass resolution. The sensitivity S/B and the significance $S/\sqrt{B}$ whose inverse is proportionnal to the relative uncertainty on the resonance, are listed in table 6.

In addition to the observation previously made, we see that the high J/ψ production rate could lead to a precise measurement, even for the ψ'. When decreasing the mass of the colliding system the signal over background ratio and the significance increase, since the combinatorial pairs disappear. On the contrary in the Υ region the sensitivities of the three systems are close since the continuum originates mainly from the heavy flavour decays, that is of the same mechanism than the signal, which is also the great interest of this continuum. Significances are also similar for the three systems.

Table 7 shows the evolution of the sentivity in the Υ mass region when the single

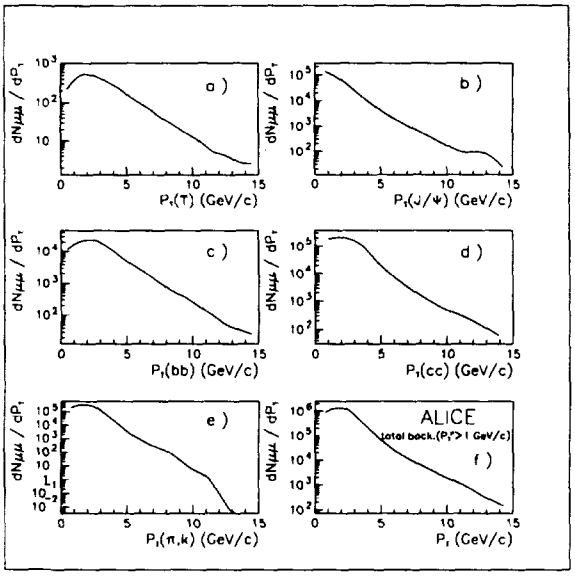

Figure 22: transversal momentum distribution of dimuon with a cut $P_T^{\mu} > 1$ GeV/cin Pb-Pb collisions with $\sqrt{s} \sim 5.5$ TeV at LHC. source: a) Υ ; b) j/ψ ; c) $b\bar{b}$; d) $c\bar{c}$; e) π, k ; f) total combinatorial background

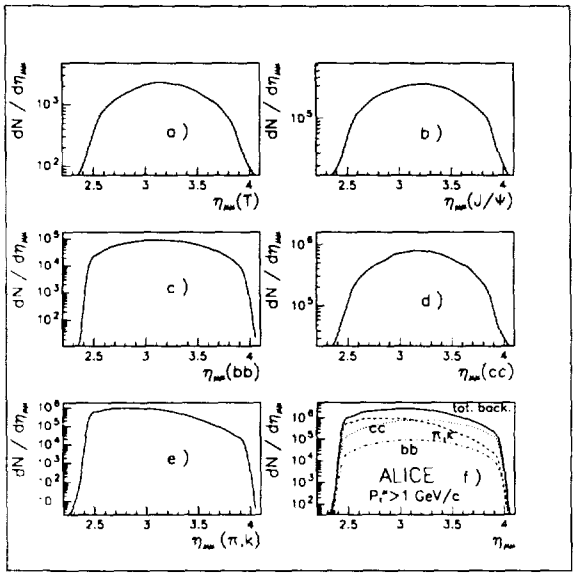

Figure 23: rapidity distribution of dimuon with a cut $P_T^{\mu} > 1$ GeV/c in Pb-Pb collisions with $\sqrt{s} \sim 5.5$ TeV at LHC. source: a) Υ ; b) j/ψ ; c) $b\bar{b}$; d) $c\bar{c}$; e) π, k ; f) total combinatorial background

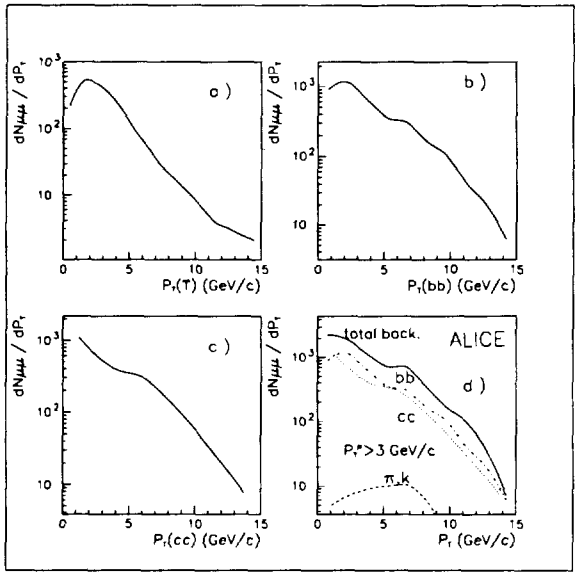

Figure 24: transversal momentum distribution of dimuon with a cut $P_T^\mu > 3$ GeV/c in Pb-Pb collisions with $\sqrt{s} \sim 5.5$ TeV at LHC. source: a) Υ ; b) $b\bar{b}$; c) $c\bar{c}$; d) total combinatorial background

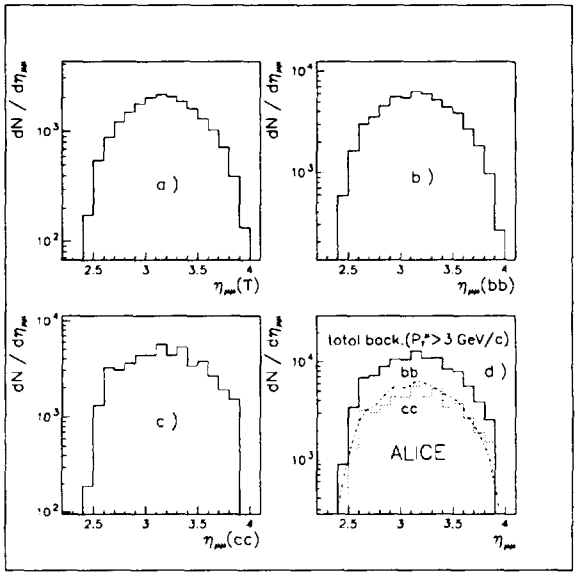

Figure 25: rapidity distribution of dimuon with a cut $P_T^\mu > 3$ GeV/c in Pb-Pb collisions with $\sqrt{s} \sim 5.5$ TeV at LHC. source: a) Υ ; b) $b\bar{b}$; c) $c\bar{c}$; d) total combinatorial background

J/ψ, ψ'									
$P_t > 1.GeV/c$ $2.4 < \eta < 4.0$	Pb-Pb $L = 10^{27} cm^{-2} s^{-1}$ in units of 10^5			Ca-Ca $L = 10^{29} cm^{-2} s^{-1}$ in units of 10^5			pp $L = 10^{30} cm^{-2} s^{-1}$ in units of 10^5		
pi , k	3.			2.5			0.005		
b - b	0.44			0.2			0.42		
c - c	4.2			1.6			0.75		
pi,k–bb	1.00			0.6			0.003		
pi,k–cc	3.4			1.9			0.01		
bb–cc	0.08			0.03					
	J/ψ	ψ'		J/ψ	ψ'		J/ψ	ψ'	
background(B)	12.2	5.2		7.	3.		1.2	0.5	
signal(S)	20.7	0.25		60.	0.7		52.	0.6	
S/B	1.7	0.05		8.5	0.23		43.	1.	
$S/\sqrt{B}$	1900	35		7000	130		15000	270	
Υ, Υ', Υ''									
$P_t > 3.0GeV/c$ $2.4 < \eta < 4.0$	Pb-Pb $L = 10^{27} cm^{-2} s^{-1}$ in units of 10^2			Ca-Ca $L = 10^{29} cm^{-2} s^{-1}$ in units of 10^2			pp $L = 10^{30} cm^{-2} s^{-1}$ in units of 10^2		
pi , k	0.03			0.02					
b - b	15.			60			38.		
c - c	15.			60.			38.		
pi,k–bb	0.25			0.15			0.0007		
pi,k–cc	0.25			0.15			0.0007		
	Υ	Υ'	Υ''	Υ	Υ'	Υ''	Υ	Υ'	Υ''
background(B)	30.5	26.	25.	120.	104.	102.	76.	65.	64.
signal(S)	81.	25.	9.5	390	129	40	160	50	18
S/B	2.6	1.	0.4	3.2	1.2	0.4	2.1	0.8	0.3
$S/\sqrt{B}$	150	50	20	360	130	40	180	60	20

Table 6: Number of pairs in the J/ψ and Υ region for all sources and combinations with various cuts. The numbers correspond to an interval of ± 100 MeV/c^2 around the resonance masses. Signal to background ratios and significance are also listed. $10^6 s$ running time for ions and 10^7 for protons have been considered.

$Pb-Pb$	$S/B(correlated+uncorrelated)$			
cut	$9.25 < M_{\mu\mu} < 9.95$	Υ	Υ'	Υ''
$P_T > 1$	1.18	1.97	0.81	0.32
$P_T > 2$	1.27	2.24	0.82	0.32
$P_T > 3$	1.49	2.5	0.97	0.39
$P_T > 4$	2.	3.2	1.4	0.5

Table 7: Comparison between the sentivities S/B for mixed muon pair production in the Υ mass domain with single muons transversal momentum cut of P_T^{μ} >1,2,3 and 4 GeV/c, in the pseudorapidity domain $2.4 < \eta < 4$ for Pb - Pb collision at 5.5 TeV.

$Pb-Pb$	$S/B(correlated)$			
cut	$9.25 < M_{\mu\mu} < 9.95$	Υ	Υ'	Υ''
$P_T > 1$	1.53	2.51	1.	0.37
$P_T > 2$	1.55	2.53	1.	0.38
$P_T > 3$	1.84	2.82	1.13	0.41
$P_T > 4$	2.4	3.6	1.79	0.55

Table 8: idem with only correlated pairs

muon transversal momentum threshold is increased from 1 to 4 GeV/c, in Pb - Pb collisions. Increasing the P_T cut selects the resonances and the sensitivity then increases. One see from table 8 where only correlated pairs are considered in the continuum that this is due to a decrease of the uncorrelated pair production.

More sophisticated cuts can be considered in order to reject the background. Two examples are given in table 9 and 10 which give the corresponding sensitivities, and figure 26 displays the transverse momentum distributions. Regarding the sensitivity the differences between the various cuts is small, except for the $P_T^{min}+0.5P_T^{max}$ cut which is increasing the J/ψ sensitivity. It is noteworthy nevertheless that such a cut applying on line on a variable of the pair could introduce biases in the background determination [26].

4.3 Comparison of Sensitivity Between Forward and Central region

Other experimental solutions have been proposed in order to measure the muon pair production in heavy ion at LHC. the solution considered here being the optimal in the forward region, the alternatives are central measurements. It has been proposed [27] to use the L3 magnet with an absorber close to the interaction point. The LHC p-p experiment CMS [28] is also measuring muons, with an absorber far from the interaction point associated to a silicon tracker close to the vertex. This inner tracker

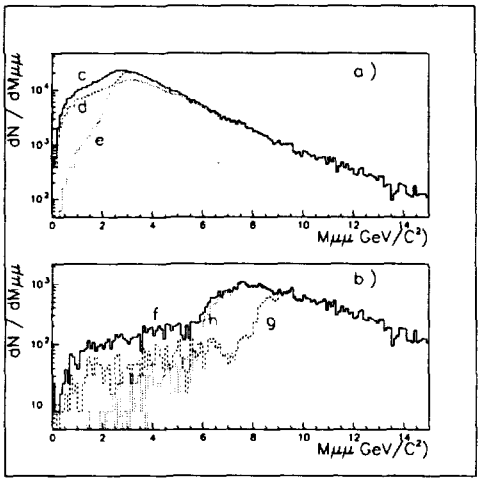

Figure 26: effect of P_T cut on the mass spectrum. three case: a) for J/ψ: c$\rightarrow$ $P_T^{\mu} > 1$; d$\rightarrow$ $P_T^{min}+0.5P_T^{max} > 2$; e$\rightarrow$ $\delta\phi > 2$, $\delta\eta > 1.6$; b) for Υ: f $\rightarrow$ $P_T^{\mu} > 3$; g$\rightarrow$ $P_T^{\mu} > 3$, $P_T^{min}+0.5P_T^{max} > 6$; h$\rightarrow$ $P_T^{\mu} > 3$, $\delta\phi > 2$, $\delta\eta > 1.6$

$Pb-Pb$ $P_T > 3$ $2.4 < \eta < 4$	S/B			
selection cut	$9.25 < M_{\mu\mu} < 9.95$	Υ	Υ'	Υ''
$P_T > 3$ *(uncorr. + corr.)*	1.49	2.56	0.97	0.39
$P_T^{min} + 0.5P_T^{max} > 6$	1.5	2.5	0.97	0.39
$\delta\phi > 2$, $\delta\eta > 1.6$	1.53	2.53	0.95	0.37

Table 9: Sensitivity for Υ measurement in an interval of $\pm$100 MeV /c^2 for Pb - Pb collision, for different muon cuts

$Pb-Pb$ $P_T > 1$ $2.4 < \eta < 4$	S/B	
selection cut	ψ	ψ'
$P_T > 1$ *(uncorr. + corr.)*	1.763	0.050
$P_T^{min} + 0.5P_T^{max} > 6$	1.990	0.051
$\delta\phi > 2$, $\delta\eta > 1.6$	1.857	0.054

Table 10: Sensitivity for $J\psi$ measurement in an interval of $\pm$100 MeV /c^2 for Pb - Pb collision, for different muon cuts

$Pb-Pb$	$S/B(correlated+uncorrelated)$								
system	*ALICE*			*L9H*			*CTR*		
cut	Υ	Υ'	Υ''	Υ	Υ'	Υ''	Υ	Υ'	Υ''
$P_T > 2$	2.241	0.819	0.332	0.887	0.342	0.136	0.184	0.076	0.032
$P_T > 3$	2.564	0.968	0.387	1.844	0.542	0.226	0.661	0.300	0.094
$P_T > 4$	3.236	1.399	0.515	3.094	0.975	0.312	1.790	0.754	0.223

Table 11: Sentivities S/B for the Υ mass domain with respect to the muon transverse momentum cut and for the three set up for Pb - Pb collision at 5.5 TeV.

allows to reach very good resolutions but has not been designed originaly for PbPb multiplicities.

In the following we consider two set ups, called L9H and CTR, which are simplified versions of the previous detectors. The goal is to investigate the effects of the changes, of the rapidity domain and of the absorber location, on the signal and background obtained. This is not supposed to give an estimate of the CMS and L3H final performances which could depend on other characteristics. For instance an improvement in resolution should have a proportionnal effect on the sensitivity due to the reduction of the relevant mass domain, when keeping the same resonances yield. In contrast this would make no change to the mixing between the various continuum sources.

The muons are measured in the pseudorapidity interval $|\eta| < 1.4$, the absorber is made of iron, 80 cm thick and starting 3 cm from the interaction point for L9H and respectively 100cm thickness and 140 cm distance for CTR.

Figure 27 to 34 display transversal momentum and pseudo-rapidity distributions for signal and background muon pairs with $P_T^\mu > 1$ and $P_T^\mu > 3$ GeV/c cuts, for the two set up. With the first P_T^μ cut, one see that already for L9H (figures 27 and 28), the light meson decays are overwhelming the other sources of continuum which were previously at the same level (figures 22 and 23). This effect gains an order of magnitude in CTR, the yield of light meson pairs increasing with the square of the ratio between the significant decay lengths of the two set ups, which are roughly the free space lengths plus the interaction length of the absorber material.

At higher dimuon masses, with the $P_T^\mu > 3$ Gev/c cut (figures 29,30, 33 and 34), the π, k decays are just starting to intervene for L9H, but are the main contribution to the continuum for CTR.

The sensitivities of Table 11 and 12 reflect quantitatively these increases of the background. Measurement of the Υ is comparable in Alice and L9H, and more difficult in CTR with a factor 3 on the background (which could be compensated by the resolution). A more critical change arises in the continuum nature, which is dominantly originating from π, k decays in the CTR case, implying a difficult extraction of the open heavy flavour component.

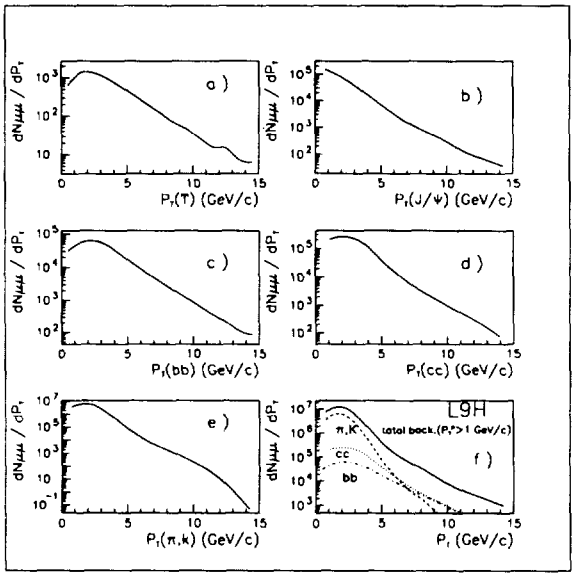

Figure 27: transversal momentum distribution of dimuon with a cut $P_T^{\mu} > 1$ GeV/c for detector L9H in Pb-Pb collisions with $\sqrt{s} \sim 5.5$ TeV . source: a) Υ ; b) j/ψ ; c) $b\bar{b}$; d) $c\bar{c}$; e) π, k ; f) total combinatorial background

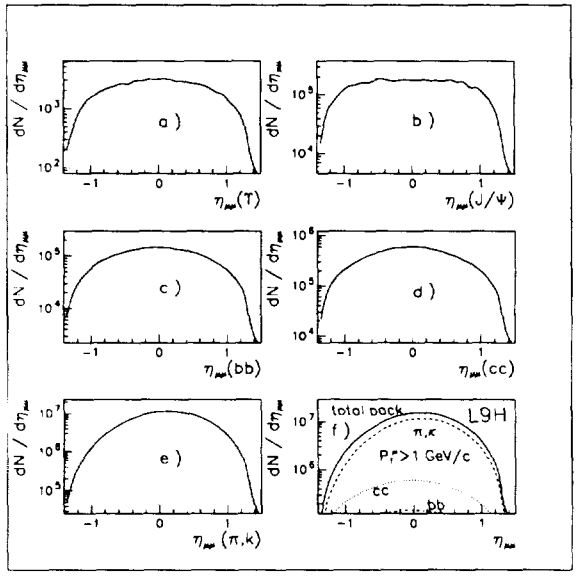

Figure 28: Idem for the rapidity distribution

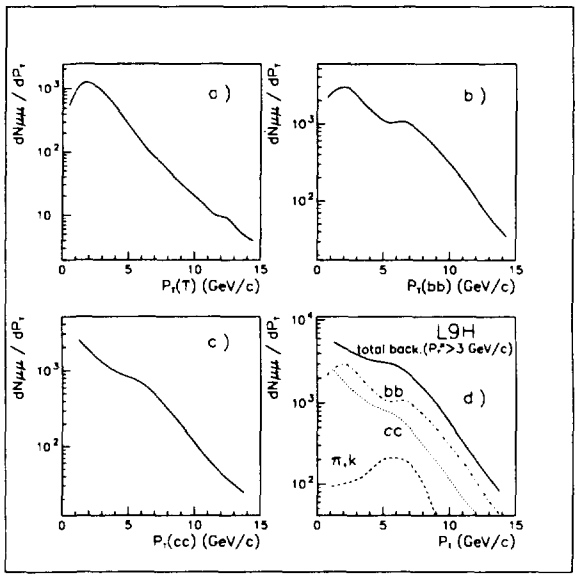

Figure 29: transversal momentum distribution of dimuon with a cut $P_T^{\mu} > 3$ GeV/c for detector L9H in Pb-Pb collisions with $\sqrt{s} \sim 5.5$ TeV . source: a) Υ; b) $b\bar{b}$; c) $c\bar{c}$; d) total combinatorial background

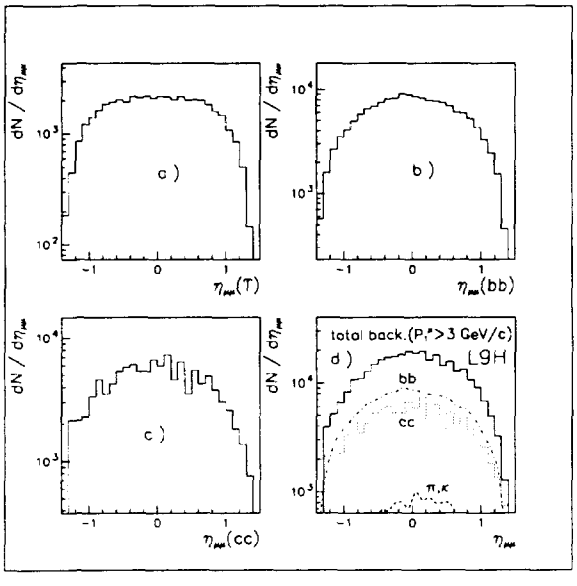

Figure 30: Idem for the rapidity distribution

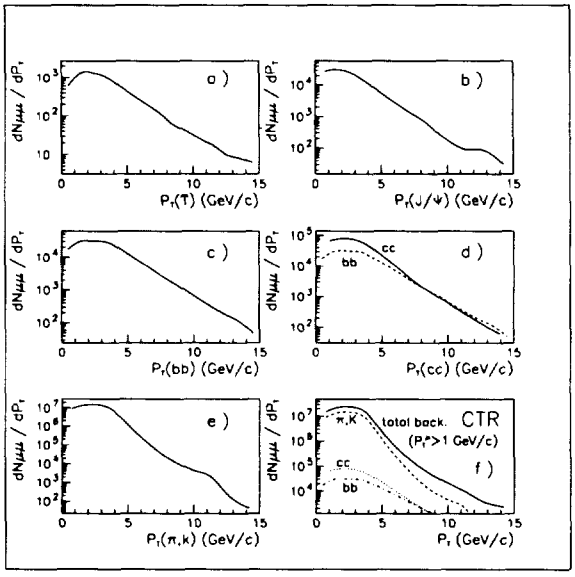

Figure 31: transversal momentum distribution of dimuon with a cut $P_T^{\mu} > 1$ GeV/c for detector CTR in Pb-Pb collisions with $\sqrt{s} \sim 5.5$ TeV . source: a) Υ; b) j/ψ; c) $b\bar{b}$; d) $c\bar{c}$; e) π, k ; f) total combinatorial background.

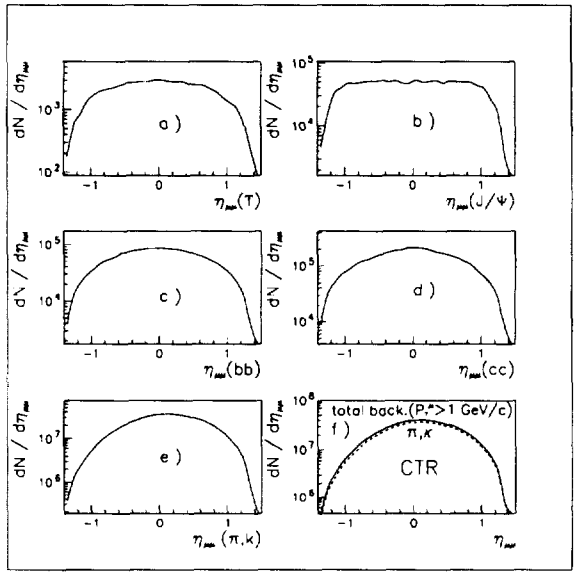

Figure 32: Idem for the rapidity distribution.

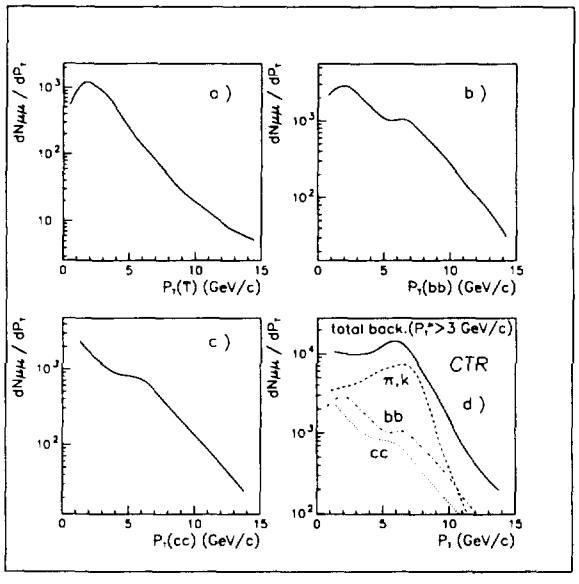

Figure 33: transversal momentum distribution of dimuon with a cut $P_T^{\mu} > 3$ GeV/c for detector CTR in Pb-Pb collisions with $\sqrt{s} \sim 5.5$ TeV . source: a) Υ ; b) $b\bar{b}$; c) $c\bar{c}$; d) total combinatorial background

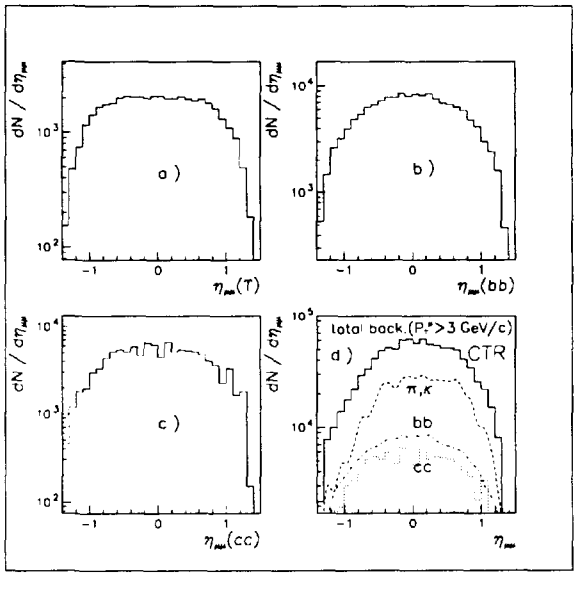

Figure 34: Idem for the rapidity distribution.

$Pb-Pb$	$S/B(correlated+uncorrelated)$		
region	$9.25 < M_{\mu\mu} < 9.95$		
system	*ALICE*	*L9H*	*CTR*
$P_T > 2$	1.268	0.512	0.116
$P_T > 3$	1.493	0.915	0.427
$P_T > 4$	1.991	1.442	1.055

Table 12: Sentivities S/B for the Υ mass domain ($9.25 < M_{\mu\mu} < 9.95$), with respect to the transversal momentum cut and for the three set up considered, for Pb - Pb collision at 5.5 TeV.

5 Conclusion

A forward muon spectrometer added to the ALICE detector will allow to study the Debye screening effect in the plasma, in particular through the measurement of the Υ. Being made in ALICE, it could permit direct correlations with the other signatures of the plasma formation, including on an event by event basis.

As for existing muon spectrometers [5] The optimitized absorber will be made of about 10 interaction lengths of carbon which could lead to a mass resolution on the 100 MeV level, allowing to separate the Υ' from Υ".

The cross section that have been considered here lead in one month running to a sufficient amount of resonances in the central Pb-Pb collisions. Their statistical significance is enhanced by the decrease of the π and K decay background, which is minimized thanks to the forward measurement and to the closeness of the absorber.

Thanks to this effect, the continuum above the Υ originates mainly from open heavy flavour production, and mostly from $b\bar{b}$ pairs, which is the ideal reference to be used in order to estimate the suppression. It is also pleasant to note that at these high masses the combinatorial effect is drastically decreasing and that this muon pair mass continuum could be directly proportional to the $b\bar{b}$ quark pair production.

A comparison with central measurement scenarii shows that, concerning the continuum, such a favourable situation is only occuring for forward measurement.

Acknowledgement

One of the authors(D.C.Zhou) is very pleased to thank M. D.Jouan very much for the hospitality and the direction extended by him during this work and during visiting at the Institut de Physique Nucleaire; and D.C. Zhou is very pleased to thank the Institut de Physique Nucleaire, the group NIM in the IPN and the CROUS de France for providing enthusiastic support for the work and the living conditions during his staying in France; he is glad to thank the colleagues of dimuon groups at Orsay, in France and at CERN for the very useful discussions about dimuon simulations, M. Y. Le Bornec, Mme N.Willis and M. J.Pouthas. I would like to thank the Director of the IPN, M. S.Gales, the director of the DRE Mme N.Frascaria, and Mmes J.MacFarlane, E.Davanture, Mrs X.Tarrago and J.Astruc for providing the helps. The financial support from the CNRS of France,the State Education Commission of China, and the National Natural Science Foundation of China(NSFC) are gratefully acknowledged.

References

[1] S.Shuryak, Phys.Rep. **61** 71(1980);
D.gross, R.Pisaarsky, and L. Yaffe, Rev. Mod. Phys.**53** 43(1981);
H.Satz,Annu.ev. Nucl. part. sci. **35** 245(1985);
L.Mclerrran,Rev. Mod. Phys. **58** 102(1986);
Xin-Nian Wang and M.Gyulassy, Phys. Rev. **D 44** 11(1991)3501.

[2] T.Matsui and H.Satz, phys. Lett. 178**B** (1986)416.

[3] F.Karsch, Proc. of the LHC Workshp, Aachen,Germany(1990),Vol. II, CERN 90-10,1141.

[4] Debye screening in Heavy Ion collisions with the ALICE Detector, CERN/LHCC/95-24, 24 April 1995

[5] C.lourenco(NA38 Collaboration), Proceeding of Qaurk Matter' 1993, Nuclear Phys. **A** 566 (1994)77c.

[6] A. Mazzoni(Helios/3 Collaboration), Proceedings of Qurk Matter'93, Nuclear Phys. **A** 566 (1994)95c

[7] N.Antoniou *et al.*, ALICE Letter of Intent, 1st March 1993,CERN/LHC 93-16.

[8] ALICE Technique Proposal, 15 december 1995, CERN/LHCC/95-71

[9] J. Sckukraft, Fifth International Conference on Nucleus-Nucleus Collisions. Taormina, Italy(1994), CERN-PPe/94-139

[10] H.Satz Charmonium production versus open charm in nuclear collisions CERN-TH-7120/93

[11] R.Gavai, D.Kharzeev, H.Satz, G.A.Schuler, K.Sridar, R.Vogt, Mod. Phys. **A**, Vol **10** 20-21(1995)3043

[12] S.Beole et al., addendum to the ALICE technical proposal, 15 octobre 1996, CERN/LHCC 96-32

[13] F.Manso,A.Baldit and P.Dupieux, Alice Internal Note 95-12.

[14] D.Jouan and D.C.Zhou, Studies for dimuon measurement in the forward region, 10/03/95, ALICE internal report ALICE 95/04

[15] K.Safarik, communication in the ALICE muon study group

[16] K.Eggert and A.Morch, Onium production in Heavy Ion Collisions at the LHC - signals and backgrounds in the two muons channel
ALICE internal report, ALICE/95-05, 15/03/95
K.Eggert,M.Morsch, ALICE Internal note 95-09.

[17] L.Lyons, Progress in particles and nuclear physics vol **7** (1981)

[18] N. Craigie, Pgys. Rep. **47** (1978)515

[19] P.Sonderegger proceeding of Large Hadron collider Workshop, Aachen 4-9 October 1990, Vol. **2**, CERN 90-10

[20] I.Sarcevic and P.Valerio preprint Arizona University AZPH-TH/93-20

[21] A.Schwarz, Phys. reports **238** 1(1994)1

[22] P.L. McGaughey *et* al., Heavy Quark Production in pp Collisions, Mod. Phys. **A**, Vol **10** 20-21(1995)2999

[23] C.Peterson et al., Phys. Rev. **D 27** (1983) 105

[24] CDF COLLAB., Phys. Rev. Lett. **61** (1988) 1819

[25] M.Bourquin and M.Gaillard, Nucl. Phys. **114** (1976)114

[26] S.Constantinescu, S.Dita, D.Jouan, determination of the error in a combinatorial estimate of the background in muon pair measurement, internal report Institut de physique nucleaire Orsay, 1996, IPNO 01-96

[27] L3H Letter of intent, Min Chen, CERN/LHCC/93-15

[28] a Compact Muon Solenoid experiment, technical proposal, CERN/LHCC/94-38

[29] R.Stock, Event by event measurements in relativistic heavy ion physic, this workshop
H.Satz, proceeding of quark matter '93, Nuclear Physics **A** 566(1994) 1c
H.Satz, proceeding of Large Hadron collider Workshop, Aachen 4-9 October 1990, vol.**1** p.188, CERN 90-10